J Solid State Electrochem (2011) 15:1971–1976
DOI 10.1007/s10008-010-1217-3

ORIGINAL PAPER

Chelation-assisted method for the preparation of cathode material $LiFePO_4$

Chengfeng Li · Ning Hua · Chenyun Wang · Xueya Kang · Tuerdi Wumair · Ying Han

Received: 9 June 2010 / Revised: 29 September 2010 / Accepted: 10 October 2010 / Published online: 27 October 2010

Abstract $LiFePO_4$/C composite cathode material is prepared by ball milling with the assistance of EDTA chelation with using water as the media of ball mill procedure. $FePO_4$ and LiOH are used as starting materials; a certain amount of glucose is used as carbon sources and reduction agent. The structure and morphology of the composite are characterized by X-ray diffraction and scanning electron microscopy. Cyclic voltammetry, AC impedance measurements, and galvanostatic charge–discharge and cycling performances are used to characterize its electrochemical properties. The results indicate that the performances of composites prepared by chelation-assisted method are much better than common ball milling method which using alcohol or acetone as the media of ball mill procedure. The stable discharge capacity of the prepared composite is 150 and 105 mAh g^{-1} at 1 and 10 C rate, respectively.

Keywords Lithium iron phosphate · Chelation-assisted method · Lithium-ion battery · Cathode material · Electrochemical performance

C. Li · N. Hua · C. Wang · X. Kang · T. Wumair · Y. Han
Xinjiang Technical Institute of Physics and Chemistry,
Chinese Academy of Sciences,
Urumuqi, Xinjiang 830011, China

C. Li
e-mail: goldenlcf@sina.com

C. Li · N. Hua · C. Wang
Graduate University of Chinese Academy of Sciences,
Beijing 100049, China

C. Li · N. Hua · C. Wang · X. Kang (✉) · T. Wumair · Y. Han
Xinjiang Key Laboratory of Electronic Information
Materials and Devices,
Urumqi, Xinjiang 830011, China
e-mail: xueyakang@yahoo.cn

Introduction

Lithium iron phosphate ($LiFePO_4$) as a kind of cathode materials has already experienced intensive investigations since it was reported by Padhi [1] and coworkers in 1997, due to its large theoretical capacity (170 mAh g^{-1}), high stability, and environmental benign [2–4]. In addition, $LiFePO_4$ has good cycle stability and a flat discharge potential of 3.4 V vs Li^+/Li. However, the slow diffusion rate of lithium ion and poor electron conductivity limit its commercial use [5, 6]. To overcoming these disadvantages, lots of work has been done and several strategies has been suggested, which could conclude as follows: (1) doping with guest cations to increase the electronic conductivity inside the particle [7–9]; (2) surface coating with conductive additive, such as C [4, 10, 11], Cu [12], and Ag [13], around $LiFePO_4$ particles to improve the electronic conductivity; and (3) minimizing the particle size and obtaining uniform size distribution by optimizing synthesis processes to shorten the distance of the bulk diffusion of Li^+ [14].

The electrochemical performance of $LiFePO_4$ is very closely related to the synthesis technique. Numerous techniques have already been used for the preparation of this materials, such as hydrothermal method [15], sol–gel method [16–19] which usually use chelating agents to hinder the aggregation of particles, and most attractive solid-state method, for its simplicity, low cost, good repeatability, and easy scale-up. Mechanochemical activation [20–22] as a modified solid-state method has received much attentions nowadays.

Here, in this paper, we adopted mechanochemical activation method using LiOH and $FePO_4 \cdot 2H_2O$ as the start materials with water as the media during ball-milling procedure. In this method, LiOH and EDTA were entirely

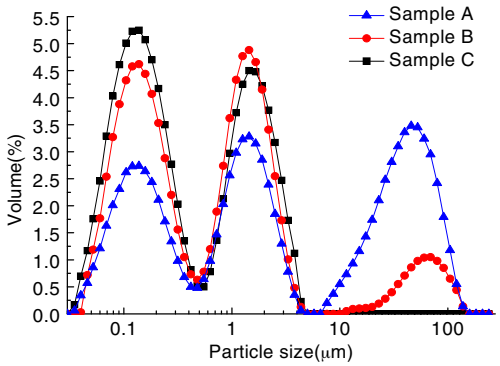

Fig. 1 Particle size distribution of the precursors after ball-milling procedure

dissolved in the water and reacted with each other (reaction (1)) [23]. Then, the excess dissolved LiOH creating a strong basic condition, and $Fe(OH)_3$ was more stable than $FePO_4$ in this condition [23]. So nano-scale amorphous $Fe(OH)_3$ was formed during ball mill procedure (reaction (2)), and EDTA as a kind of strong chelating agents [24] could link with the surface Fe atoms to prevent the aggregation of particles. In addition, Fe atoms on the surface of nanocrystals could be peeled off by EDTA forming chelated compounds [22, 23, 25] during milling action (reaction (3)). These combined actions could decrease the crystal size farther. The solid-chelating reaction could be described as follows (X = EDTA):

$$4LiOH + H4X \rightleftarrows Li4X + 4H2O \quad (1)$$

$$3LiOH + FePO4 \rightleftarrows Fe(OH)3 + Li3PO4 \quad (2)$$

$$FePO4 + Li4X \rightleftarrows LiFeX + Li3PO4 \quad (3)$$

Furthermore, the carbonized products of EDTA could also prevent the aggregation during sintered procedure.

Although certain amount of work have been done about this material by using chelating agent such as citric acid in mechanochemical activation method [22, 26, 27], there are only several reports involve using water as the media of ball-milling and using EDTA as the chelating agent during their experiments up to now. The use of water as ball-milling media facilitates the solution reaction in the system during ball milling. Water as the most effective solvent could combine ball mill action with ionic reactions in water, such as chelation reaction, during ball milling.

In this study, we have compared this chelation assisted method with the tradition mechanochemical activation which usually using alcohol or acetone as the media of ball-mill procedure. The structure, morphology, and electrochemical properties of the prepared samples are investigated in detail.

Experimental

Preparation of samples

Three different samples were prepared by ball milling: they were sample A (without chelating agent), sample B (contain 5 wt.% EDTA as chelating agent), sample C (contain 10 wt.% EDTA as chelating agent). Each sample was prepared through following procedures.

Sample A was prepared by using glucose as reductive agent and carbon source. Stoichiometric amount of $FePO_4 \cdot 2H_2O$ and $LiOH \cdot H_2O$ were ball milled with 15 wt.% glucose for 7 h in alcohol in a planetary miller with nylon vessels and ZrO_2 balls, using ball-to-powder ratio of 4:1 and a rotation speed of 350 rpm. The ball-milling procedure experienced seven periods. Each one contains two parts: first rotated clockwise for 0.5 h and then rotated anticlockwise for another 0.5 h. The milled powder was dried at 70 °C in a dry oven and then sintered at 700 °C for 10 h burying in a sealed box filled with acetylene black. The arrangement in the sealed box could be seen in Fig. 10, and the sealed box was placed in a furnace without using any atmosphere.

Samples B and C were prepared by ball milling stoichiometric amount of $FePO_4 \cdot 2H_2O$ and $LiOH \cdot H_2O$ with 5 and 10 wt.% EDTA for 7 h in deionized water, respectively. After the powder was dried, 15 wt.% glucose was added while grinding the powder in mortar. Other procedures and conditions were same as the preparation of sample A.

Sample characterization

In order to investigate the effect of EDTA addition in the system, optical particle size analyzer (Mastersizer 2000, England) was

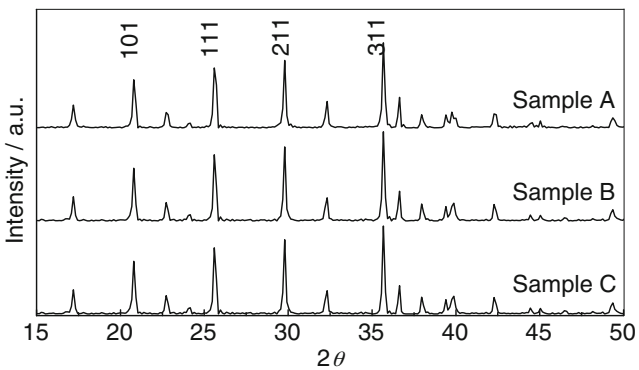

Fig. 2 XRD patterns of the samples

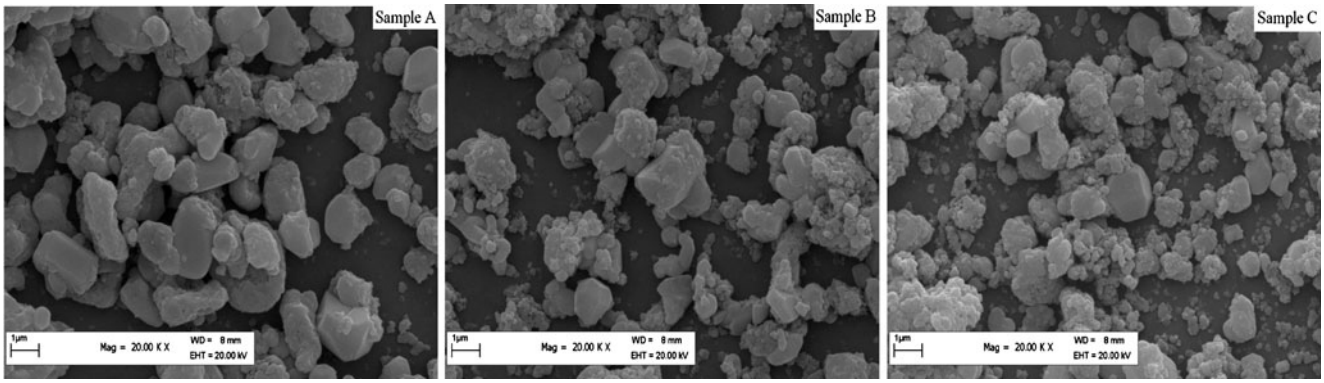

Fig. 3 SEM photographs of the samples

used to investigate the particle size distribution of the precursors after ball-mill procedure. The phase structures of the samples were investigated by X-ray diffraction (XRD, RINT-2500V, Rigaku Co.) using Cu Kα radiation (λ=1.5418 Å) in the range of 15–50° with a scanning rate of 2° per minute. The morphologies of particles were observed by scanning electron microscope (LEO-1430VP). In order to investigate the carbon distribution in the samples, HRTEM (JEM-2010) was used in this work.

To test the electrochemical performances, the cathode was prepared by spreading the cathode slurry (80 wt.% of the active material) onto an aluminum foil followed by drying in vacuum at 120 °C for 12 h. The cells (CR2025) were assembled in an argon filled glove-box using lithium metal foil as the counter electrode. The electrolyte was 1.0 mol dm^{-3} $LiPF_6$ in a mixture of ethyl carbonate, diethyl carbonate, and dimethyl carbonate (volume ratio 1:1:1). Electrochemical performances of $LiFePO_4$ were investigated by using CR2025 coin-type cell. The cells were charged and discharged between 2.3 and 4.3 V at room temperature on a charge/discharge apparatus (BTS-51, Neware, China). Cyclic voltammetry (CV) and electrochemical impedance spectroscopy (EIS) were conducted by using a CHI650 electrochemical working station. The sinusoidal excitation voltage of EIS was 10 mV and the frequency range was between 10^5 and 10^{-2} Hz.

Results and discussion

In order to investigate the effect of EDTA addition in the system, optical particle size analyzer (Mastersizer 2000, England) was used to characterize the particle size distribution of the precursors after ball-mill procedure. As shown in Fig. 1, samples A and B exhibited three peaks, but sample C had only two peaks. The peak located between 10~100 μm was absence for sample C, and the peak value of sample A at this region was much larger than sample B. This phenomenon indicated the large particles can be pulverized by the combined actions containing EDTA chelation and milling action. Furthermore, the peak values around 0.1 and 1 μm for samples B and C were

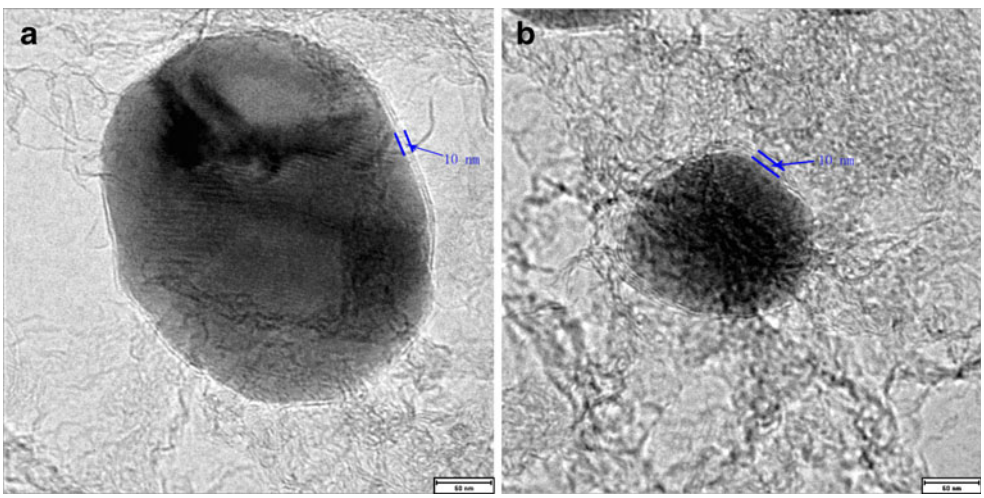

Fig. 4 HRTEM images of **a** sample A and **b** sample C

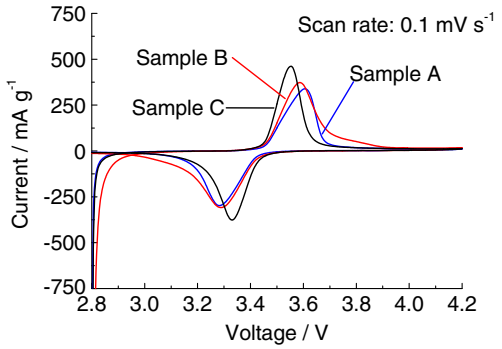

Fig. 5 CV profiles of the samples at 0.1 mV s^{-1}

larger than sample A, which denoted the larger proportion of particles with size around 0.1 and 1 μm range. These instances illustrated the size reduction effect of EDTA in the ball-milling system. Then, the precursors were sintered at 700 °C to form $LiFePO_4$/C composites.

The X-ray diffraction patterns of the three samples were shown in Fig. 2. All peaks could be indexed as olivine phase with an ordered orthorhombic structure belonging to the space group Pnma (JCPDS No. 40–1499). The absence of any other signals indicated there were no high-content impurities and the residual carbon decomposed from glucose to EDTA was amorphous in the $LiFePO_4$/C composite. The results from XRD patterns demonstrated this method was suitable for produce pure $LiFePO_4$. In this work, Fe^{3+} in the precursor was reduced to Fe^{2+} with the help of strong reductive atmosphere, which was generated by EDTA and glucose pyrolysis.

When the carbon precursors were sintered at high temperature, its decomposition would happen while the forming of $LiFePO_4$ phase. The decomposed carbon coupled with $LiFePO_4$ form $LiFePO_4$/C composite. The carbon content of the three samples were measured according to literature [28], the results were 6.1%, 6.6%, 6.9% for sample A, B, C, respectively. Clearly, the more EDTA was added, the more carbon was formed. This can be ascribed to the remnant carbon after the pyrolysis of EDTA.

Scanning electron microscopy (SEM) was used to investigate the morphology of the particles. Figure 3 showed the results of SEM. It was obvious that the proportion of particles with the size of hundreds nanometers in samples B and C were much more than sample A. It illustrated that our chelation-assisted method could effectively decrease the particles size of $LiFePO_4$/C composite. Further, it was clearly in the photos that the more EDTA was added, the larger proportion of nano-sized particles was formed in the produced cathode materials. It illustrated that EDTA took an important role in the decreasing of the particles. Because as a kind of strong chelating agents [24], EDTA could link with the surface Fe atoms to prevent the aggregation of particles. Furthermore, the residual carbon decomposed from EDTA stayed at the particle interval hindered the aggregation during the sintered procedure.

In order to investigate the carbon distribution in the composites, HRTEM was used in this work. Figure 4 presented the HRTEM images of samples A and C. It could be seen in the images that the residual carbon was amorphous and distributed homogeneously around $LiFePO_4$ particles. And $LiFePO_4$ particles were completely coated by carbon layer to form a core-shell structure. The thickness of carbon layer for both samples was about 10 nm which could enhance the conductivity of the composites without hindered the insertion/desertion of lithium ions.

CV was conducted to investigating the electrochemical properties of the three samples. The CV profiles of the three samples at the scan rate of 0.1 mV s^{-1} were displayed in Fig. 5. All of them presented a pair of redox peaks around 3.44 V vs Li^+/Li, but the profiles of samples B and C were more symmetric. As revealed in Fig. 5, the potential intervals between anodic peak and cathodic peak of samples B and C were smaller than sample A indicating an enhancement of electrochemical properties for samples B and C. The largest peak current for sample C denoted the largest effective diffusion constant [29]. The CV curves of sample C at different scan rate were shown in Fig. 6. As the sweeping rate was raised, the oxidation peak shifted higher, and the reduction peak shifted lower.

To evaluated electrode impedance, Fig. 7a presented the Nyquist plots of the three samples at the same charge/discharge state. An intercept at the Z' axis in high frequency corresponded to the ohmic resistance (R_e), which represented the resistance of the electrolyte. The semicircle in the middle frequency range indicated the charge transfer resistance (R_{ct}). The inclined line in the low frequency represented the Warburg impedance (Z_w), which was associated with lithium–ion diffusion in the $LiFePO_4$ particles. Obviously, the charge transfer resistance (R_{ct}) had the following sequence: sample A > sample B > sample

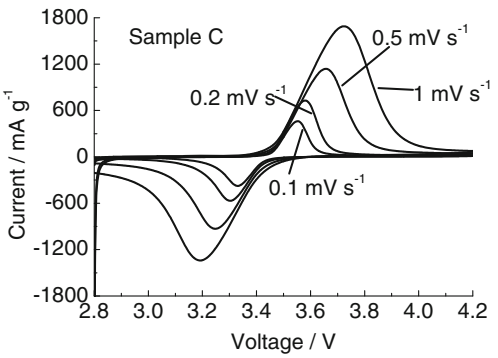

Fig. 6 The CV curves of sample C at the different scan rates

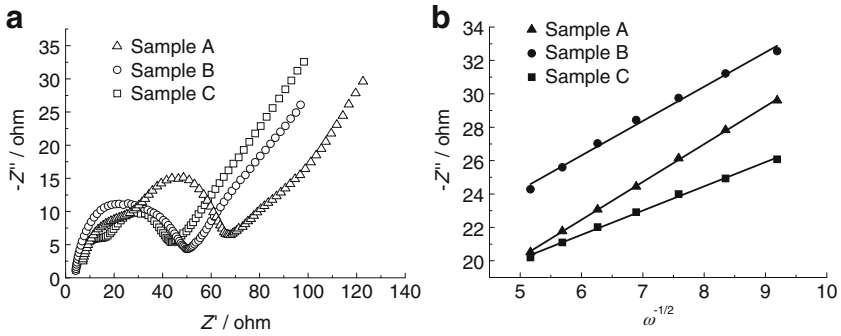

Fig. 7 **a** Nyquist plots of the samples. **b** The relationship between Z'' and $\omega^{-1/2}$ for the three samples

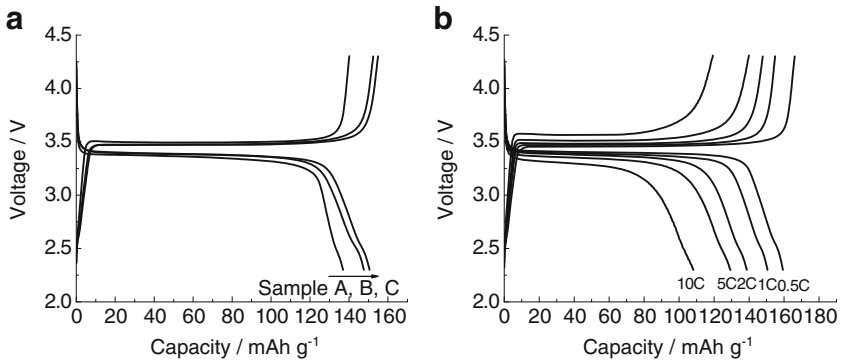

Fig. 8 **a** The charge/discharge curves of the samples at 1 C. **b** Charge/discharge tests at different C rates of sample C

C, indicated the electrode/electrolyte interface reaction could process more convenience for sample B and C. According to the literature [30], the lithium diffusion coefficient could be calculated by combining the following two equations:

$$D = \frac{R^2T^2}{2n^4F^4C^2\sigma^2} \tag{4}$$

$$Z'' = \sigma\omega^{-1/2} \tag{5}$$

where D is lithium-ion diffusion coefficients, R is the gas constant, T is the absolute temperature, n is the number of electrons per molecule during oxidization, F is the Faraday constant, C is the concentration of lithium ion, and σ is the Warburg factor which could be obtained by Eq. (5). Thus, the lithium-ion diffusion coefficient was inverse proportion to σ^2. Figure 7b showed the relationship between Z'' and square root of frequency $\omega^{-1/2}$ in the low frequency region, the value of σ could be obtained from the slop. So, a sequence of lithium diffusion coefficients could be got as follows: sample A < sample B < sample C. This result may be the benefit of the larger proportion of nano-sized particles.

The galvanostatic charge/discharge performances of the three samples were presented in Fig. 8. As shown in Fig. 8a, the discharge capacities of 136.9, 147.6, and 150.6 mAh g^{-1} were obtained at 1 C rate for sample A, sample B, and sample C, respectively. These results accompanied with the performances of CV and EIS indicated the improvement of the electrochemical properties of $LiFePO_4$ after EDTA chelation during ball-mill procedure. Figure 8b was the charge/discharge performances of sample C at different C rates, a discharge capacity of 105.5 mAh g^{-1} could be still obtained at 10 C, denoting good rate performances.

The cycling profiles of the three samples at different C rates were displayed in Fig. 9. Both samples B and C

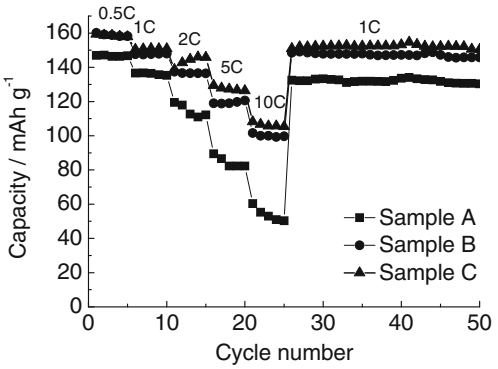

Fig. 9 Cycling profiles of the three samples at different C rates

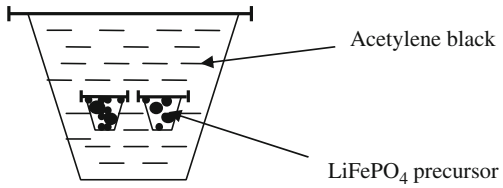

Fig. 10 The equipment for synthesizing $LiFePO_4$

indicated better cycling profiles with little capacity fading at high current densities. The EDTA chelation-assisted method not only enhanced the capacity of $LiFePO_4$ but also improved its cycle stability at high-current densities. All the results above illustrated the improvement of $LiFePO_4$ with the EDTA chelation (Fig. 10).

Conclusion

In this work, the $LiFePO_4$ cathode material has been successfully prepared by EDTA chelation-assisted method. The XRD results indicated the well crystallized $LiFePO_4$ was formed. The SEM revealed that nano-sized particles became dominating after EDTA chelation during ball mill procedure. Both CV, EIS, and galvanostatic charge/discharge tests results denoted an enhancement of the electrochemical properties by this method. They also revealed an increasing of the discharge capacities especially at high current densities while the increasing of EDTA amount. All of them illuminated the efficiency of this method. These enhancements could be ascribed to the larger proportion of nano-sized particles which was benefit from chelation of EDTA. In this method, three reasons could be concluded to clarify this enhancement of electrochemical properties. First, EDTA rapidly chelated with surface Fe atoms while a new surface was created by physical mill to hinder the aggregation of nanocrystals. Second, LiOH was entirely dissolved in the water creating a basic condition, and $Fe(OH)_3$ was more stable than $FePO_4$ in this condition. So nano-scale amorphous $Fe(OH)_3$ was formed during ball-mill procedure, and EDTA as a kind of strong chelating agents could link with the surface Fe atoms to prevent the aggregation of particles. Third, Fe atoms on the surface of nanocrystals could be peeled off by the chelation of EDTA during milling action to decrease the crystal size farther and the carbonized products of EDTA could also prevent the aggregation during sintered procedure. In this work, the electrochemical performances indicated that the more EDTA was added, the better the performances were. In addition, this method had lots of advantageous for large-scale production, such as simple processes and low cost of raw materials especially using water as the media of ball milling.

References

1. Padhi AK, Nanjundaswamy KS, Goodenough JB (1997) J Electrochem Soc 144:1188–1194
2. Andersson AS, Thomas JO (2001) J Power Sources 97:498–502
3. Arnold G, Garche J, Hemmer R, Strobele S, Vogler C, Wohlfahrt-Mehrens A (2003) J Power Sources 119:247–251
4. Wang YG, Wang YR, Hosono EJ, Wang KX, Zhou HS (2008) Angew Chem Int Ed 47:7461–7465
5. Nishimura S, Kobayashi G, Ohoyama K, Kanno R, Yashima M, Yamada A (2008) Nat Mater 7:707–711
6. Hu YS, Guo YG, Dominko R, Gaberscek M, Jamnik J, Maier J (2007) Adv Mater 19:1963, −+
7. Chung SY, Bloking JT, Chiang YM (2002) Nat Mater 1:123–128
8. Wang GX, Bewlay S, Yao J, Ahn JH, Dou SX, Liu HK (2004) Electrochem Solid State 7:A503–A506
9. Liao XZ, He YS, Ma ZF, Zhang XM, Wang L (2007) J Power Sources 174:720–725
10. Yang SF, Song YN, Zavalij PY, Whittingham MS (2002) Electrochem Commun 4:239–244
11. Bewlay SL, Konstantinov K, Wang GX, Dou SX, Liu HK (2004) Mater Lett 58:1788–1791
12. Croce F, Epifanio AD, Hassoun J, Deptula A, Olczac T, Scrosati B (2002) Electrochem Solid State Lett 5:A47–A50
13. Park KS, Son JT, Chung HT, Kim SJ, Lee CH, Kang KT, Kim HG (2004) Solid State Commun 129:311–314
14. Gaberscek M, Dominko R, Jamnik J (2007) Electrochem Commun 9:2778–2783
15. Jin EM, Jin B, Jun DK, Park KH, Gu HB, Kim KW (2008) J Power Sources 178:801–806
16. Kim JK, Choi JW, Chauhan GS, Ahn JH, Hwang GC, Choi JB, Ahn HJ (2008) Electrochim Acta 53:8258–8264
17. Arumugam D, Kalaignan GP, Manisankar P (2009) J Solid State Electrochem 13:301–307
18. Liu H, Xie JY, Wang K (2008) J Alloys Compd 459:521–525
19. Yu F, Zhang JJ, Yang YF, Song GZ (2009) J Mater Chem 19:9121–9125
20. Huang B, Zheng XD, Jia DM, Lu M (2010) Electrochim Acta 55:1227–1231
21. Fey GT-K, Chen YG, Kao HM (2009) J Power Sources 189:169–178
22. Zhang D, Yu X, Wang YF, Cai R, Shao ZP, Liao XZ, Ma ZF (2009) J Electrochem Soc 156:A802–A808
23. Zumdahl SS (1998) Chemical Principles. Houghton Mifflin, Boston
24. Aelterman P, Versichele M, Genettello E, Verbeken K, Verstraete W (2009) Electrochim Acta 54:5754–5760
25. Sawyer DT, Paulsen PJ (1959) J Am Chem Soc 81:816–820
26. Xu Y, Lu Y, Yan L, Yang Z, Yang R (2006) J Power Sources 160:570–576
27. Liu J, Wang J, Yan X, Zhang X, Yang G, Jalbout AF, Wang R (2009) Electrochim Acta 24:5656–5659
28. Beninati S, Damen L, Mastragostino M (2008) J Power Sources 180:875–879
29. Nakamura T, Sakumoto K, Okamoto M, Seki S, Kobayashi Y, Takeuchi T, Tabuchi M, Yamada Y (2007) J Power Sources 174:435–441
30. Gao F, Tang ZY (2008) Electrochim Acta 53:5071–5075